Physics – Uspekhi **46** (6) 657 – 663 (2003)

METHODOLOGICAL NOTES PACS numbers: **72.15.–v**, **74.25.–q**, **74.72.–h**

Nonlinear effects and domain instability in oxide ceramics

V F Khirnyĭ, A A Kozlovskiĭ

DOI: 10.1070/PU2003v046n06ABEH001259

Contents

Abstract. **Nonlinear current – voltage characteristics and domain instabilities are discussed for bulk (granular) ceramic samples at high electric current densities in the range from room temperature to premelting temperature.**

1. Introduction

Bulk studies of electrical conductivity (σ) nonlinearities and domain instabilities have been primarily carried out on semiconductors [1, 2] and metals [3, 4]. Domain formation in granular sample characterized by tunneling conductance came under study [5, 6] only after the discovery of high-temperature superconductivity (HTSC) [7]. Subsequent studies [8 – 10] of domain instabilities in oxide ceramics not only revealed much about the way mobile charge carriers behave, are produced, and decrease in number, but also provided insight into why an electric current I passing through such materials changes their conductivity [11 – 20]. In the present paper, unusual aspects of the nonlinear variation of σ versus I in the normal state of HTSC ceramics are also considered.

2. Electrical conductivity nonlinearities in bulk solids

The current – voltage characteristics of homogeneous bulk conductors become nonlinear when the energy distribution of the charge carriers differs from the equilibrium distribution because of a strong electric field E [1]. The uniform distribution of the field E in a conductor becomes unstable and gives rise to a temperature-electric domain (TED), a mobile local region with increased values of E, energy dissipation JE (J being the current density), and the temperature T. In the $I-V$ characteristic, a nonlinear portion with negative differential conductivity (NDC), $\sigma = \mathrm{d}J/\mathrm{d}E < 0$, appears. The electric current density J in a 'one-dimensional' isotropic conducting medium, with unipolar conductivity and the **J** and **E** vectors collinear, is expressed by [2]

$$\mathbf{J} = en\mu\mathbf{E} = \frac{e^2 n\tau_{\mathrm{e}}}{m}\,\mathbf{E}\,. \tag{1}$$

Here e is the charge of the carrier, and μ, τ_{e}, and m are the carrier's mobility, (isotropic) relaxation time, and mass, respectively. The condition $\sigma < 0$ is fulfilled if either the drift velocity of the charge carriers, or their density, or both decrease with increasing E. NDC then results from the equilibrium disturbance in the system of carriers, without the lattice experiencing Joule heating. Note, however, that the warming of the lattice affects the shape of the $I-V$ curve and alters the conditions under which a TED occurs [3, 4]. A change in the lattice temperature changes the rate of electron – phonon collisions, thus establishing a relation between τ_{e} and E [3, 4].

From Eqn (1) it follows that as τ_{e} decreases with increasing E, the $\sigma < 0$ regime will also occur for $\mathrm{d}(\tau_{\mathrm{e}}E)/\mathrm{d}E < 0$ [3]. Conditions for the existence of NDC with $\mathrm{d}(\tau E)/\mathrm{d}E < 0$ are determined by examining the thermal conduction equation [3, 4] written for a one-dimensional current-carrying sample oriented along the x axis [3]:

$$C_v\,\frac{\partial T}{\partial t} + \frac{\partial q}{\partial x} = JE - Q(T)\,, \tag{2}$$

where C_v is the specific heat of the sample; t is time; q is the heat flow density; $Q(T) = Q/d$ is the ratio of the heat flow

V F Khirnyĭ, **A A Kozlovskiĭ** Institute for Single Crystals, The National Academy of Sciences of Ukraine,
prosp. Lenina 60, 61001 Khar'kov, Ukraine
Tel. (+380-572) 30 83 11
Fax (+380-572) 32 02 73
E-mail: khirnyi@isc.kharkov.com

Received 3 June 2002, revised 18 September 2002
Uspekhi Fizicheskikh Nauk **173** (6) 679 – 685 (2003)
Translated by E G Strel'chenko; edited by M V Magnitskaya

across the sample surface in the direction of its normal, to the sample thickness d; and Q is the flow per unit area of the surface. If the electrical neutrality condition $\operatorname{div}\mathbf{J} = 0$ is fulfilled then, substituting J and q into Eqn (2) and using the relevant transport equations [21] we obtain [3]

$$C_v \frac{\partial T}{\partial t} + JT \frac{\mathrm{d}}{\mathrm{d}T}\left(\frac{\alpha}{\sigma}\frac{\partial T}{\partial x}\right) - k\frac{\partial^2 T}{\partial x^2} = \sigma(T)\,E^2 - Q(T)\,, \tag{3}$$

where $\alpha = S_\mathrm{d}\sigma(T)$, S_d is the differential thermoelectromotive force, and k is the thermal conductivity.

In the prescribed current regime

$$\frac{U}{\int \mathrm{d}x[\sigma(T)]^{-1}} = J = \mathrm{const}\,,$$

the TED is unstable, whereas in the prescribed voltage regime

$$J\int \mathrm{d}x\big[\sigma(T)\big]^{-1} = U = \mathrm{const}\,,$$

the TED is stable [1]. In the latter case, for $T = \mathrm{const}$, Eqn (3) has the following solution uniform over the sample [3]:

$$E^2 = \frac{Q(T)}{\sigma(T)}\,. \tag{4}$$

Condition (4) establishes the relations between E and T and between τ_e and E. Hence [3]

$$\mathbf{J} = \sigma\big[T(E)\big]\mathbf{E} \tag{5}$$

and

$$\frac{\mathrm{d}J}{\mathrm{d}E} = \frac{(Q\sigma)'_T}{(Q/\sigma)'_T\sigma}\,. \tag{6}$$

For normal metals $\sigma(Q/\sigma)'_T > 0$, and $\mathrm{d}J/\mathrm{d}E < 0$ if $(Q\sigma)'_T < 0$ [3]. This is possible only if the T-dependent part of the conductivity $\sigma(T)$ — the one due to the electron–photon interaction — is larger than the T-independent part of σ_0 [3]. The nonlinearity mechanism outlined above applies to sufficiently pure, bulk, and perfect metallic samples at $T < 0.1\,\Theta_\mathrm{D}$ (where Θ_D is the Debye temperature). NDC arises from the decrease in σ with increasing E due to the electron–phonon interaction [3, 4].

Thus, the appearance of NDC and a TED is due to concentration-, recombination-, and temperature-related mechanisms, as well as other mechanisms, either separately or in combination [1–4].

3. Methods for obtaining negative differential conductivity

There are several methods available for achieving NDC in solids. Since the most common instability regime is the temperature-electrical one [1–4], it is with this particular regime in mind that we will consider DC methods for obtaining NDC in metals [3]. From expression (6) it follows that a region with $(Q\sigma)'_T < 0$ exists (see Fig. 1 reproduced from Ref. [4]). As the current is increased, the sample, originally at a temperature T_1, is heated to $T = T_3$ — without going through the region $\mathrm{d}J/\mathrm{d}E < 0$ if the I–V curve is measured in the prescribed current regime (horizontal line). The sample can even burn out in this process.

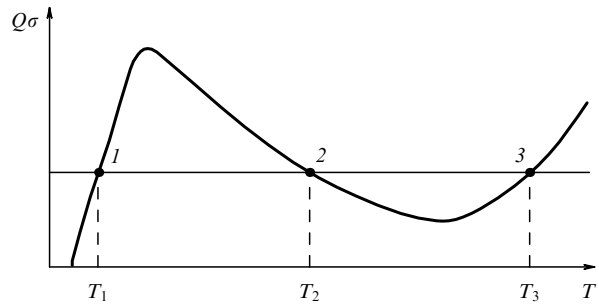

Figure 1. Functions $Q(T)\sigma(T)$.

When operating in the regime in which voltage across the sample is prescribed [3], the drop in the voltage U_h in the heated region, of size L_h and with electrical resistance R_h, should be considered separately from that in the remaining, cold part of the sample, with U_c, L_c and R_c, respectively. As the current rises from zero, temperature fluctuations are initially small, $\delta T \ll T_0$ and $R_\mathrm{c} \ll R_\mathrm{h}$. The voltage drop across the sample's hot part is [3]

$$U_\mathrm{h} = E_\mathrm{h}L_\mathrm{h} \cong U\frac{R_\mathrm{h}}{R_\mathrm{c}}$$

and that across its cold part is

$$U_\mathrm{c} = U\left(1 - \frac{R_\mathrm{h}}{R_\mathrm{c}}\right) \cong U\,.$$

The current I depends practically linearly on U, and

$$J = \sigma_\mathrm{c}E_\mathrm{c} \cong U\frac{\sigma_\mathrm{c}}{L_\mathrm{c}}\,.$$

From this it follows that the thermal balance condition

$$U^2\,\frac{\sigma_\mathrm{c}^2}{L_\mathrm{c}^2} = Q_\mathrm{h}\sigma_\mathrm{h} \cong \mathrm{const} \tag{7}$$

remains the same as for the regime with a current source, when $J \cong \mathrm{const}$. As long as $R_\mathrm{h} \ll R_\mathrm{c}$, the temperature will keep rising — as it does in the prescribed current regime. As the current increases still further and the sample is further heated, the point may be reached when the inequality $R_\mathrm{h} \ll R_\mathrm{c}$ is violated and its opposite, $R_\mathrm{h} \gg R_\mathrm{c}$, holds instead. The voltage across the hot part of the sample increases, and in the ideal (limiting) case may become practically equal to that across the entire sample, i. e., $U_\mathrm{h} \cong U$, giving rise to a TED in it. The voltage drop across the cold part of the sample,

$$U_\mathrm{c} \cong U\,\frac{\sigma_\mathrm{h}}{\sigma_\mathrm{c}}\,,$$

follows from the electrical neutrality condition as

$$J_\mathrm{c} \cong J_\mathrm{h} = U\,\frac{\sigma_\mathrm{h}}{L_\mathrm{h}}\,.$$

If the condition $(Q\sigma)' < 0$ still holds (as it must as before), the current will decrease in the heated region and in the whole of the sample. The temperature therefore will cease to rise when the quantity Q/σ reaches a value for which the condition

$$\frac{U_\mathrm{h}^2}{L_\mathrm{h}^2} = \frac{Q}{\sigma}\,,$$

is fulfilled, analogous to Eqn (7) but with σ_c and L_c replaced respectively by σ_h and L_h (power is now dissipated in the hot part of the sample).

For the stable operation of a direct current scheme it is necessary that the power U^2/R_i dissipated in the external resistance R_i would exceed the power U^2/R dissipated in the negative resistance of the sample R, a condition which is fulfilled when $R_i < |R|$. This stability criterion was obtained based on the load line concept [3, 22].

4. Necessary conditions for the study of current–voltage characteristics with negative differential conductivity

To detect a TED, it is necessary to secure appropriate conditions for its observation, namely, to choose a heat removal regime so as to make the inequality

$$\frac{\mathrm{d}(Q/\sigma)}{\mathrm{d}T} < 0$$

easier to fulfil. There are several methods for removing heat from an object under study [3]: by radiation, by convective (free or forced) heat exchange with the gaseous environment, or by heat conduction along the leads. Radiative heat removal, in which the heat flow per unit area of the surface is

$$q(T) \propto T^4 ,$$

is ineffective in comparison with the free convective heat exchange, in which the heat removal power is

$$W(T) \propto d^{3\eta-2}(T - T_0)^{1+\eta} ,$$

where $\eta = 0.125-0.133$ and T_0 is the ambient temperature [23]. Using the equation

$$(j^*)^2 \frac{\mathrm{d}\rho}{\mathrm{d}T} = \frac{\mathrm{d}W(T)}{\mathrm{d}T}$$

to determine the domain formation current I^*, the following relation between I^*, the sample thickness d, and the ambient temperature T_0 is obtained [23]:

$$I^* \propto d^{1+1.5\eta}(T - T_0)^{0.5(1+\eta)} .$$

The calculations of Ref. [23] agree both qualitatively and quantitatively with the experimental $I^*(d)$ dependence.

Heat removal through copper leads, with $q(T) \propto (T^2 - T_0^2)$, cannot compete with convective heat removal through the gaseous environment at high temperatures either.

5. Nonlinear effects in the electrical conductivity of HTSC ceramics

Osip'yan et al. [5] and Bobrov et al. [6] reported the observation of a TED in the orthorhombic-structure HTSC ceramics $Y_1Ba_2Cu_3O_{7-x}$, $Ho_1Ba_2Cu_3O_{7-x}$ ($T_c \cong 96.6$ K), $Er_1Ba_2Cu_3O_{7-x}$ ($T_c \cong 66$ K), and $La_{1.6}Sr_{0.4}CuO_4$ ($T_c \cong 37$ K), where T_c is a critical temperature.

The samples, $3 \times 3 \times 40$ mm^3 in size, were prepared by hot compression molding of powders. During the course of the experiments, the samples usually were in the air, with an electrical current flowing through them. When the current density $J \cong 10^6$ A m^{-2} and $T \cong 400\,^\circ$C were reached, a TED showed up as a shining strip on the sample, the current decreased, and there was a drop in temperature in regions of the sample remote from the TED. The properties of the TED were studied at a temperature $T_d \cong 1000$ K as determined by an infrared imager. In the DC regime, the TED moved toward the negative pole of the source of electromotive force (emf) at a velocity of $v \cong 10^{-1}$ m h^{-1}. The velocity depended on the sample structure, decreased as the heat removal conditions improved, and increased toward higher temperatures due to the temperature gradient. The motion of the TED reversed direction as the polarity of the leads was changed. At the same time, the TED was observed to be pinned near the current contacts, in sample inhomogeneities, and in local heat removal regions. The pinning effect could be overcome by applying an external temperature gradient.

During the TED formation process, the loss of oxygen at the TED location led to the formation of a tetragonal phase and caused an increase in the electrical resistivity R locally. From the X-ray diffraction data it followed that the tetragonal phase at the center of the domain, where $T_d \cong 779\,^\circ$C, transformed to an orthorhombic phase towards the domain edges, where $T \cong 200\,^\circ$C. After repeated passage of the TED through the sample, the fraction of the tetragonal phase in it increased, the oxygen content decreased, and T_c dropped off.

The observed phenomenon may be due to the nonlinear $R(T)$ dependence in the sample's region where $T \cong 400\,^\circ$C [8]. The motion of the TED was explained by a model in which the TED, in a sense, pumps the oxygen ions from neighboring regions of the ceramic into its own central part. Because of the effect of the electrical field, the oxygen ion concentration is different on different sides of the TED, thus pushing it into the lower-concentration region.

The motion of the TED along ceramic HTSC samples is a modified technique of the crucibleless zone melting. In order to realize this technique, the properties of both the TED itself and the ceramic samples along which it moved, were examined [8–10].

5.1 Temperature-concentration instabilities in the formation of temperature-electric domains

The $YBa_2Cu_3O_{7-x}$ ceramic samples used in the studies [8–10] were prepared [24] in the form of disks 0.1 m in diameter using the hot compression molding of the powder ($\cong 97\,\%$ mol $YBa_2Cu_3O_{7-x}$) at temperatures from 600 to 7500 °C. The disks were cut into bars which ranged between 0.03 m and 0.1 m in length and between 1×3 mm^2 and 6×6 mm^2 in cross section.

Of the more than 50 samples studied, some had a rhombic and others a tetragonal structure. The phase which crystallizes into the rhombic crystal system was obtained by holding the samples at 900–930 °C for 1 to 2 hours and then cooling them in the furnace first at a rate of 50 °C h^{-1} to 350 °C, and then arbitrarily. The tetragonal phase formed after the ceramics were held at 900–930 °C and then taken out of the furnace and cooled on metallic or ceramic stands at a rate of 20–50 °C min^{-1} [24].

The electrical conductivity of yttrium ceramics depends significantly on the concentration of electric charge carriers (holes) in the sample [25]:

$$\sigma_p = n_p q_p \mu_p , \tag{8}$$

where n_p, q_p, and μ_p are the hole concentration, charge, and mobility, respectively. On warming from room temperature

to $T \cong 350\,^{\circ}\mathrm{C}$, σ_{p} drops linearly with temperature. As the temperature increases further, a sharp increase in the electrical resistivity R in the temperature range from $400\,^{\circ}\mathrm{C}$ to $\cong 675\,^{\circ}\mathrm{C}$ is observed [6] as a result of the bulk desorption of oxygen from the ceramics [25]. The desorption (absorption) of oxygen on heating (cooling) can be written in the form [25]

$$\mathrm{O}_0 + 2\mathrm{h} \rightleftarrows \mathrm{V}_0 + \frac{1}{2}\mathrm{O}_2\,, \tag{9}$$

where O_0 is the neutrally occupied site of oxygen O(1), h is a hole, V_0 a vacancy, and O_2 an oxygen molecule.

According to Eqn (9), an oxygen atom diffuses through O(5) sites through exchange with a vacancy. Oxygen loss by the ceramics heated in the indicated temperature range causes a decrease in the hole concentration n_{p} and in the conductivity σ_{p}, i.e., leads to NDC on the $I-V$ curve. A TED in yttrium ceramics results from a temperate-concentration instability that develops in the uniform distribution of the field E. The fact that a TED disappears when samples are subjected to air blowing or placed in a liquid nitrogen vapor confirms the crucial role of convective heat removal through the exchange with the gaseous environment as a means of securing the condition $\mathrm{d}(Q\sigma)/\mathrm{d}T < 0$.

5.2 The effect of external conditions on TED properties

According to Refs [5, 6], the surrounding atmosphere affects the properties of a TED. In an oxygen enriched medium the velocity of a TED increased from when the sample was in the air. In a medium with little or no oxygen — in a helium or nitrogen atmosphere — a TED was observed to narrow, its velocity significantly decreased, and the sample rapidly burned out. In a vacuum, a TED showed up as a narrow shining strip and at its location the sample immediately decomposed.

The domain temperature T_{d} increased with increasing U (decreasing I) on the falling portion of the $I-V$ curve [8–10]. The quantity T_{d} could be regulated in the range from $\cong 400\,^{\circ}\mathrm{C}$ to $\cong 1000\,^{\circ}\mathrm{C}$. As T_{d} increased, the width of the TED increased and its velocity v decreased. In Figure 2 are shown the temperature-versus-time curves for a TED moving along the sample [8]. The arrow indicates the direction of TED motion. The samples were horizontally oriented. In vertically oriented samples the value of v increased as the TED moved upwards and decreased as it moved downwards. A minimum value $v \cong 0.1$ m h^{-1} was achieved in the study.

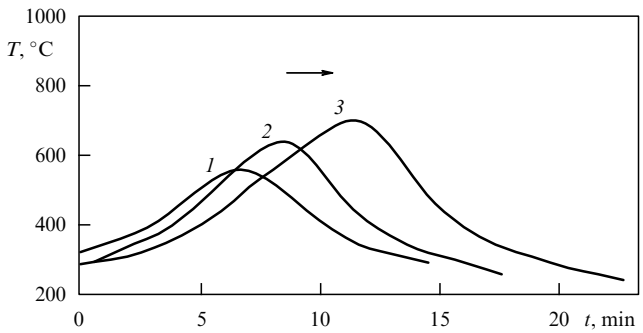

Figure 2. Variation of temperature with time for a TED moving along an yttrium ceramic sample. Curves *1*, *2*, and *3* are for the following sample voltages: $U_1 = 2.5$ V; $U_2 = 2.7$ V; and $U_3 = 3.0$ V.

TED velocity changes were due to three forces that act on a TED and make it perform a stationary motion along the sample: the diffusion force F_{D}; the drift force $F_{\mathrm{q}} = -\mathrm{grad}\,\mu_{\mathrm{p}}$ [22], which makes positive charge carriers (holes) drift toward the negative pole of the voltage source; and the thermal force $F_{\mathrm{T}} = T\,\mathrm{grad}\,(1/T)$ [22], due to the fact that in a non-uniformly heated conductor a current can flow even at $E = 0$. The relationship between these three forces has been analyzed in Ref. [8].

It was predicted [1] that the magnetic field affects the properties of TEDs in semiconductors. According to Ref. [8], a transverse magnetic field of the order of 1 T does not affect the TED velocity, whereas a longitudinal field does. A TED was accelerated (decelerated) when the direction to the southern (northern) pole coincided with that to the sample's contact connected to the positive pole of the emf source. A magnetic field $B \cong 1$ T stopped the motion of the TED. To produce the field, a superconducting warm-bore solenoid was used.

5.3 Spatial TED dynamics and the theoretical results

Although the behavior of TEDs in metals and ceramics have much in common, there are some differences. The following properties of TEDs in ceramics are analogous to those predicted in Ref. [4] for metallic conductors:

(1) When a current is sent through a sample initially, the dependence of T on E, Eqn (4), is determined from the heat balance condition [4]:

$$JE = d_{\mathrm{g}}^{-1} q(T)\,, \qquad J = \sigma(T)E\,, \tag{10}$$

where d_{g} is a geometry factor.

(2) A TED ceased its motion when encountering inhomogeneities.

(3) The velocity of a TED remained virtually unchanged when the sample's cross section area was varied from 3 mm^2 to 36 mm^2.

(4) A TED may be produced by changing the geometry factor.

The following features distinguish TEDs in ceramics from those in metals:

(1) In metals a TED appeared due to the fact that R increases with the field E because of the electron–phonon interaction; in ceramics, due to the increased concentration of mobile charge carriers, i. e., holes.

(2) In ceramics a TED always moved from the positive to the negative electrode of the emf source. In metals, reversing the polarity changed only the speed of TED motion [23], not its direction.

(3) According to Ref. [4], the velocity of a TED in metals is

$$v \propto \alpha(T_{\mathrm{d}})\left[q(T_{\mathrm{d}})\sigma(T_{\mathrm{d}})\right]^{0.5} C_V^{-1}(T_{\mathrm{d}})\, d_{\mathrm{g}}^{-1} \cong 1-0.1\ \mathrm{mm\,s^{-1}}\,,$$

whereas in yttrium ceramics $v \cong 10^{-2}$ mm s^{-1}.

In Reference [8], to describe the behavior of TED in ceramics, Maxwell's equations and the charge continuity equation have been reduced to a single equation,

$$\dot{E} = DE_{xx} + \mu(E)\,E\left(E_x - \frac{4\pi e}{\varepsilon}\,N\right) + \frac{c}{\varepsilon}\,\mathrm{rot}\,\mathbf{H} - \int \mathrm{d}x\,\dot{E}(x)\,, \tag{11}$$

which describes the motion of a field $E(x)$ switching wave. To account for the temperature gradient due to the convective heat transfer, Eqn (11) was complemented by the heat

conduction equation [26]

$$\frac{\partial T}{\partial t} = D_t T_{xx} + \mu\big[T(E)\big]E^2 - \beta\nabla T - \alpha_T(T - T^*)\,. \qquad (12)$$

Here $\dot{E}$ is the first derivative of E with respect to time t, D is the diffusion coefficient of the charge carriers, E_{xx} is the second derivative of E with respect to x, μ is the mobility of the electric charges, E_x is the first derivative of E with respect to x, ε is the dielectric constant, D_t is the thermal diffusion coefficient, T_{xx} is the second derivative of T with respect to x, β is the convective constant, α_{T} is the heat-transfer coefficient, T^* is the ambient temperature, and N the total number of charge carriers. The model reproduces all aspects of TED behavior.

As an example to illustrate this point, the relative scale plot in Fig. 3 shows the TED formation process and presents numerical simulation results for TED motion.

As seen in Fig. 3a, the $T(x)$ dependence is as in Fig. 2. In addition to the shape of the $T(x)$ function, the dependences of n on E and x are shown in Fig. 3a. Note also that the time dependence of the heat release power P (upper curve) agrees well with experiment [8]; in particular, the curve decreases and levels off to remain constant in the stationary regime (Fig. 3b). Plots which show the conservation of the total charge N in the system and the drop in the voltage U over time are also given in Fig. 3b.

In Figure 3c the phase portrait of the set of Eqns (11) and (12) in the E, E_x plane, with a clearly seen stationary attractor (dashed line), is shown. In the inset to the figure, the same attractor is shown as an $I-V$ curve for the system under study. And in Fig. 3d the quantity U is plotted for all TED points as a function of time and of the TED position in the sample. The sample was oriented horizontally, and the convection contributed nothing to TED motion, i.e., $\beta = 0$. Similar results were also obtained when convective heat exchange was taken into account, both for $\beta > 0$ and $\beta < 0$ [8].

5.4 The effect of a temperature-electric domain on the nonlinearity of the current – voltage characteristic

After repeated passages of a TED along the sample, its $I-V$ characteristic changed its shape (Fig. 4) — unlike semiconductors and metals, where no such change was observed. By analogy with the studies [11 – 20], which showed that the passage of electrical current changed the cation and anion composition of a sample, it was assumed [8 – 10] that the TED formation process involves electrochemical reactions and ion displacements. To find out what caused changes in the $I-V$ curve shape, electrical, X-ray, and magnetic measurements were carried out, electron microscopy studies were conducted, and the chemical composition of the samples was determined, as were deviations from stoichiometry with respect to oxygen [8 – 10].

Thus, it was observed that after a TED with a local temperature $T_{\mathrm{d}} \leqslant 900\,^{\circ}\mathrm{C}$ passed along a sample, the sample lost a small fraction of its oxygen, which increased the volume of the unit cell and distorted it. To determine the decrease in oxygen content, the compleximetric titration technique was used.

The electron microscopy studies of the transverse and longitudinal cross sections of TED stopping regions using the scanning electron microscope JSM-820 with an X-ray microanalysis system Link AN 10.000 revealed a considerable increase in the density of a ceramic and showed no change in its cation composition.

Along with these measurements, chemical composition measurements were carried out at premelting temperatures $T_{\mathrm{d}} \cong 1000\,^{\circ}\mathrm{C}$ along a sample divided into 5-mm sections. The results are illustrated by plots in Fig. 5, which show how the

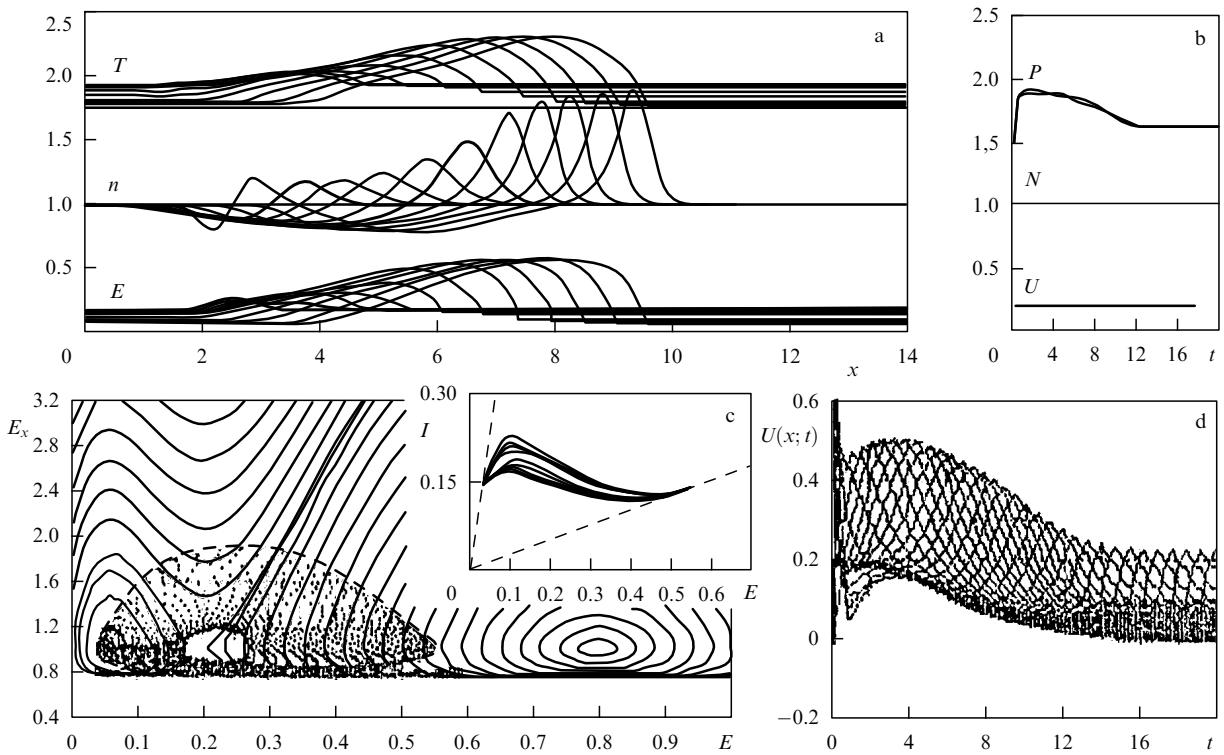

Figure 3. Numerical simulation results for TED motion (relative scale).

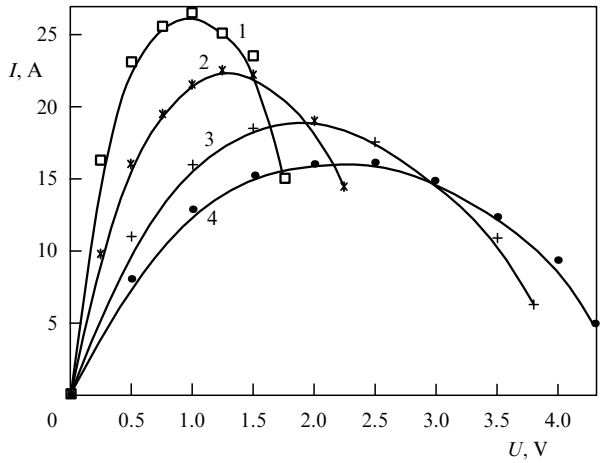

Figure 4. $I-V$ curve shape change in an yttrium sample following repeated TED 'treatments'. Figures on the curves indicate the number of TED runs.

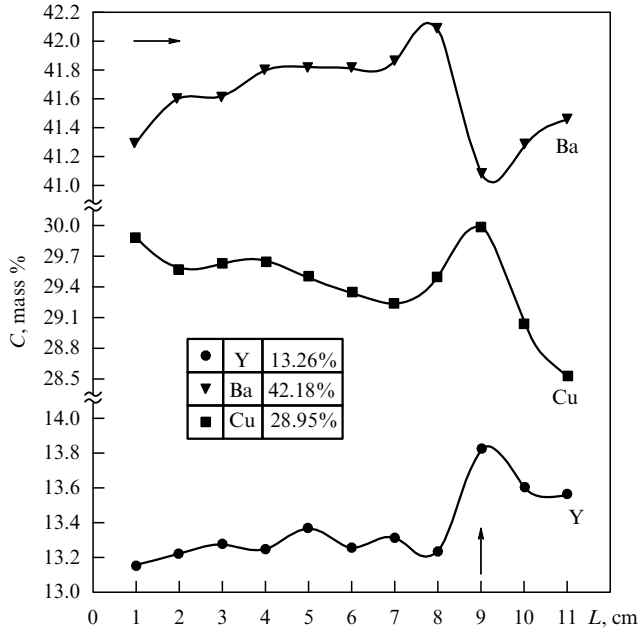

Figure 5. Change in the content of Y, Ba, and Cu along a sample after it has been 'treated' with a TED at a temperature $T_d = 950\,°C$.

content of Y, Cu, and Ba ions changes along the sample. The horizontal arrow indicates the direction of motion of a TED which moved four times in the same direction; the vertical arrow indicates the domain's stopping region. To create a TED at one and the same place, a small heating furnace was used. The picture seen in Fig. 5 is similar to that obtained for the zone melting process. In the inset, data on the chemical composition of the initial sample are presented [9, 10].

The degradation of samples after TED runs was studied by measuring the complex magnetic susceptibility $\chi_{ac} = \chi' + i\chi''$, where χ' and χ'' are the real and imaginary parts, respectively. It was found that the absolute value of $\chi'(T)$ decreases, reflecting the decreased content of the superconducting phase in the sample (see also Refs [5, 6]). Depending on the value of T_d and on the number of processing cycles performed, the volume of the remaining superconducting phase varied from 80% to 5%. Figure 6

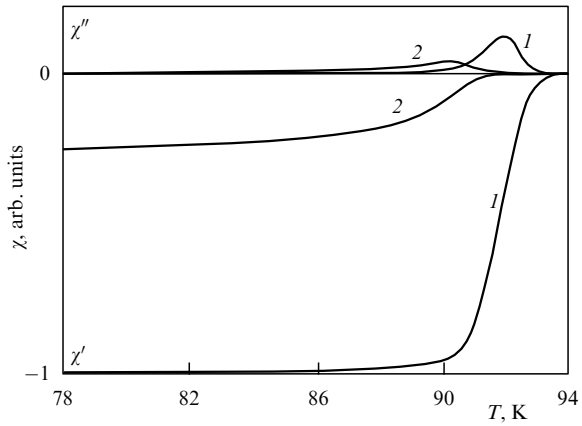

Figure 6. Change in the $\chi'(T)$ and $\chi''(T)$ dependences in a TED treated sample. Curves *1* and *2* are obtained before and after the treatment, respectively.

shows the change in the shape of $\chi'(T)$ and $\chi''(T)$ following the treatment of a sample with a TED with $T_d = 950 \pm 50\,°C$. It is seen that the curves $\chi'(T)$ are similar to those measured in samples with a reduced oxygen index [8, 9]. The samples reestablished their superconducting properties when annealed in an oxygen atmosphere. If the treatment was carried out in an oxygen atmosphere, annealing was not needed [27]. Furthermore, samples with a tetragonal crystal structure restored their superconducting properties partially after a TED treatment [9, 10].

6. Conclusion

Thus, the study of nonlinear effects in granular materials (oxide ceramics) has provided new insights into the phenomenon of domain instability in bulk samples. It is found that a temperature-concentration instability of an electric field at high current densities gives rise to a temperature-electric domain which performs a stationary motion along the sample from the positive electrode end. The properties of the domain were explained using a model [8] in which the formation and motion of an electric field switching wave is considered for a uniform medium since it was shown [8 – 10] that as far as the TED is concerned, a granular medium is uniform. TED displacement velocities can only be affected by large-size strong-heat-release inhomogeneities [26] — ones that pin the TED. Whether a TED appears or not in a ceramic sample does not depend on what type of crystal lattice the sample has. The TED treatment of samples with the hexagonal lattice led to the partial restoration of their superconducting properties.

After a short-duration passage of a high-density current through the TED location (a region heated to $T \cong 1000\,°C$ locally), a change in sample stoichiometry was observed, akin to the material composition change taking place during the zone melting process.

References

1. Volkov A F, Kogan Sh M *Usp. Fiz. Nauk* **96** 633 (1968) [*Sov. Phys. Usp.* **11** 881 (1969)]
2. Bonch-Bruevich V L, Zvyagin I P, Mironov A G *Domennaya Elektricheskaya Neustoĭchivost' v Poluprovodnikakh* (Domain Electrical Instabilities in Semiconductors) (Moscow: Nauka, 1972) [Translated into English (New York: Consultants Bureau, 1975)]

3. Tszyan Yu N, *Thesis for Doctorate of Physico-Mathematical Sciences* (Khar'kov: B.I. Verkin Institute for Low Temperature Physics and Engineering of the USSR Academy of Sciences, 1983) p. 230
4. Kadigrobov A M, Slutskin A A, Krivosheĭ I V *Zh. Eksp. Teor. Fiz.* **87** 1314 (1984) [*Sov. Phys. JETP* **60** 754 (1984)]
5. Osip'yan Yu A et al. *Pis'ma Zh. Eksp. Teor. Fiz.* **47** 257 (1988) [*JETP Lett.* **47** 310 (1988)]
6. Bobrov V S et al., in *Fiziko-Khimiya i Tekhnologiya VTSP-Materialov* (Physics, Chemistry, and Technology of HTSC materials) (Ed. N P Lyakishev) (Moscow: Nauka, 1989) p. 117
7. Bednorz J G, Müller K A *Z. Phys. B* **64** 189 (1986)
8. Khirnyĭ V F et al. *Sverkhprovodimost'*: *Fiz., Khim., Tekhnol.* **7** 575 (1994)
9. Seminozhenko V P et al. *Functional Mater.* **1** 19 (1994)
10. Khirnyĭ V F et al. *Fiz. Khim. Obrabot. Mater.* (5) 66 (1995)
11. Rajan R G, Parameswaran P, Jambunathan J B *Bull. Electrochem.* **5** 761 (1989)
12. Panasyuk B A et al., in *Tezisy Dokladov II Vsesoyuz. Konf. po VTSP, Kiev, 25 – 29 Sent. 1989* (Proc. of the 11th All-Union Conference on HTSCs, Abstracts) (Kiev, 1989) p. 13
13. Prokhorov A M et al. *Pis'ma Zh. Eksp. Teor. Fiz.* **51** 132 (1990) [*JETP Lett.* **51** 148 (1990)]
14. Sumarokov V N et al. *Sverkhprovodimost'*: *Fiz., Khim., Tekhnol.* **3** 2081 (1990) [*Supercond. Phys. Chem. Technol.* **3** 1527 (1990)]
15. Nefedov V I et al. *Sverkhprovodimost'*: *Fiz., Khim., Tekhnol.* **4** 987 (1991) [*Supercond. Phys. Chem. Technol.* **4** 898 (1991)]
16. Nefedov V I et al. *Mod. Phys. Lett. B* **5** 1019 (1991)
17. Nefedov V I, Val'kovskiĭ M D, Sokolov A N *Sverkhprovodimost'*: *Fiz., Khim., Tekhnol.* **5** 1081 (1992) [*Supercond. Phys. Chem. Technol.* **5** 1078 (1992)]
18. Mitin A V, Alekseevskiĭ N E, Khlybov E P *Sverkhprovodimost'*: *Fiz., Khim., Tekhnol.* **5** 290 (1992) [*Supercond. Phys. Chem. Technol.* **5** 286 (1992)]
19. Mitin A V, Alekseevskii N E, Khlybov E P *Physica C* **199** 351 (1992)
20. Jia Y Q, Liu X W, Jin M Z *Phys. Lett. A* **155** 214 (1991)
21. Ziman J M *Electrons and Phonons*: *The Theory of Transport Phenomena in Solids* (Oxford: Clarendon Press, 1960) [Translated into Russian (Moscow: IL, 1962)]
22. Ridley B K *Proc. Phys. Soc. London* **82** 954 (1963)
23. Abramov G I et al. *Pis'ma Zh. Eksp. Teor. Fiz.* **37** 453 (1983) [*JETP Lett.* **37** 535 (1983)]
24. Kotok L A et al. *Bull. Mater. Sci.* **14** 167 (1991)
25. Lagraff J R, Han P D, Payne D A *Physica C* **169** 355 (1990)
26. Gurevich A Vl, Mints R G *Usp. Fiz. Nauk* **142** 61 (1984) [*Sov. Phys. Usp.* **27** 19 (1984)]
27. Khirnyi V F, Chykanova I N *Functional Mater.* **3** 225 (1996)